Polymer 49 (2008) 5410–5416

Contents lists available at ScienceDirect

Polymer

journal homepage: www.elsevier.com/locate/polymer

Molecular shape recognition-structure correlation in a phenylalanine-based polymer–silica composite by surface-initiated atom transfer radical polymerization

Miklós Czaun, M. Mizanur Rahman, Makoto Takafuji, Hirotaka Ihara*

Applied Chemistry and Biochemistry, Kumamoto University, 2-39-1 Kurokami, Kumamoto 860-8555, Japan

ARTICLE INFO

Article history:
Received 5 June 2008
Received in revised form 7 October 2008
Accepted 10 October 2008
Available online 1 November 2008

Keywords:
Atom transfer radical polymerization
Inorganic–organic composite
Molecular shape recognition

ABSTRACT

A polymerizable L-phenylalanine-derived monomer (*N'*-octadecyl-*N*$^{\alpha}$[4-(acryloyloxy)-butanoyl]-L-phenylalanineamide (**3**)) has been newly synthesized and characterized. We reported an advanced approach to molecular shape recognitive hybrid materials that involves immobilization of radical initiator on mesoporous silica particles (average diameter, pore size and surface area are 4 μm, 12 nm, and 300 $m^2 g^{-1}$, respectively) and surface-initiated atom transfer radical polymerization of monomer **3** from initiator-grafted particles. All samples were characterized by elemental analysis, thermogravimetric analysis, diffuse reflectance infrared Fourier transform spectroscopy, solid state NMR measurements (^{13}C CP/MAS NMR and ^{29}Si CP/MAS NMR), differential scanning calorimetry and scanning electron microscopy. The obtained polymer–silica hybrid material was used as a stationary phase for reversed-phase high performance liquid chromatography (RP-HPLC) to investigate its molecular shape recognition ability towards polycyclic aromatic hydrocarbons (PAHs). The new composite material showed better planarity selectivity than octadecylsilane stationary phase as a conventional RP-HPLC packing material and also enhanced linearity selectivity compared with the recently reported poly(*N'*-octadecyl-*N*$^{\alpha}$-(4-vinyl)-benzoyl-L-phenylalanineamide)-grafted silica. Such selectivity enhancement can be attributed to the combination of hydrophobic effect due to octadecyl chains and multiply carbonyl π–benzene π interaction between the amide groups of the stationary phase and delocalized electrons of PAHs.

1. Introduction

Hybrid inorganic–organic composite materials have attracted increasing attention because of their potential ability to combine the properties of inorganic materials (e.g. optical and magnetic behaviors, conductivity) with the properties of organic compounds (solubility in organic solvents, insulator) [1–4]. Coating of polymers on a solid inorganic surface is a subject of a great interest in, e.g. catalysis [5], colloid stabilization [6] biomolecule immobilization [7] adhesion in composite materials [8] furthermore, hybrid materials are the most widely used stationary phases in liquid chromatography [9]. Aiming at tailoring the surface properties of inorganic particles, ultrathin films have been prepared from large variety of polymers [10]. In numerous systems polymeric brushes are prepared from block copolymers where one of the blocks is strongly adsorbed to the surface with the other block forming the brush layer [11]. Since the interaction between the polymer and the surface is usually not so strong (van der Waals forces, hydrogen bonding), desorption can occur upon exposure of the hybrid to a good solvent or using higher temperature [12].

To overcome the problems related to the instability of the inorganic–polymer hybrids, stronger interaction has to be established between the inorganic surface and the polymer shell, in other words, the macromolecules must be covalently bound to the surface. Covalent immobilization of polymers onto porous surfaces can be achieved in two ways including "grafting to" approach (1) [13–15] which involves the condensation of an end functionalized polymer with the reactive surface groups of the substrate (often OH groups). However, the immobilization of preformed polymer onto surface often leads to low grafting density because polymer chains have to diffuse against an increasing concentration gradient [16]. "Grafting from" approach (2) starting with the initiator fixed on the surface is expected to give high grafting densities because the diffusion of monomer molecules into the chain end is not hindered by the already grafted polymers [17,18]. Grafting from methods can be sub-divided into two groups based on the applied polymerization method: (1) conventional polymerization and (2) controlled polymerization techniques. The methods in the first group [19] belong to surface-initiated processes, and consequently, fairly high grafting density can be achieved, do not provide control on the

* Corresponding author. Tel.: +81 96 342 3661; fax: +81 96 342 3662.
E-mail address: ihara@kumamoto-u.ac.jp (H. Ihara).

0032-3861/$ – see front matter © 2008 Elsevier Ltd. All rights reserved.
doi:10.1016/j.polymer.2008.10.017

molecular weight and molecular weight distribution neither a facility to perform block copolymerization. Since the propagation of radicals is not controlled and polymer chains grow inside the pores very fast, these polymerization reactions may result in the blocking of the pore system and polymer brushes with high polydispersity. A slower and controlled process can make the rate of the polymerization less dependent on the diffusion of monomer molecules to the active sites providing a more uniform film thickness and decreasing the probability of blocking pore orifices [20].

To circumvent the above mentioned deficiencies of conventional polymerization reactions, controlled (“living”) radical polymerization techniques (CRP) were developed [21,22]. Atom transfer radical polymerization (ATRP) has been the most rapidly developing method among CRP since its discovery by Matyjaszewski and Sawamoto [23], owing to its high tolerance to numerous functional groups present in monomers. ATRP processes usually require a homolytically cleavable alkyl halide (dormant initiator) and a metal complex in its lower oxidation state as a catalyst. The initiation step, namely the reversible halogen atom transfer from the dormant initiator to activator complex provides a propagating radical and a deactivator complex. As a result of low radical concentration the rate of termination reactions is significantly lower than in conventional radical polymerization reactions thus surface-initiated ATRP does not only improve the grafting density of the attached polymers but may provide polymer chains with controlled molecular weight and molecular weight distribution.

The most extensively studied inorganic–organic hybrids are organically modified mesoporus silicates that have been obtained by the grafting of organic molecules such as long chain alkyl silanes [24] or polymers [25] and applied as stationary phases for liquid chromatography. In C8/C18-type reversed phase (RP) liquid chromatography the interaction between stationary phase and analytes is primarily based on hydrophobic effect with the alkyl chains of the *n*-alkyl chain ligands as well as silanophylic interactions with the non-functionalized accessible surface silanol groups. It was reported by Ohmact et al. that free silanol groups may also interact with the delocalized electrons of polycyclic aromatic hydrocarbon (PAH) analytes via OH–π interaction contributing to the enhanced selectivity [26]. It is noteworthy that introduction of any π–π active functionality to the stationary phase may also have a significant influence on the chromatographic selectivity of compounds with extended π-electron system. For example, the presence of carbonyl groups in poly(octadecyl acrylate)-grafted silica (Sil-ODA$_n$) provided enhanced shape selectivity for PAHs via carbonyl π–benzene π interaction compare with the commercially available octadecylsilane (ODS) column [27]. Furthermore, we have recently reported on the molecular shape recognition of two π-electron containing polymer hybrids such as poly(*N*′-octadecyl-*N*$^{\alpha}$-(4-vinyl)-benzoyl-L-phenylalanineamide)-grafted silica (Sil-poly(Phe-St)) [28] and poly(4-vinylpyridine)-grafted silica (Sil-VP$_n$) [29] towards PAHs. The monomer unit of the phenylalanine-derived stationary phase involves two benzene rings and two carbonyl groups providing driving force for π–π interaction and carbonyl π interaction respectively. As we expected, both Sil-poly(Phe-St) and Sil-VP$_n$ stationary phases showed generally better molecular shape selectivity than ODS but while Sil-poly(Phe-St) gave fairly good linearity selectivity, Sil-VP$_n$ had excellent planarity and poor linearity selectivity. Latter is due to the lack of driving force in VP$_n$ to form any ordered structure that is essential for discriminating linearity. As a part of our systematic studies aiming at understanding how the structure of polymers in silica–polymer hybrids affects the molecular recognition ability, we have designed a new monomer involving a flexible spacer between the amino acid and the polymerizable group. Moreover, this monomer also involves an octadecyl chain providing hydrophobicity and three carbonyl functional groups to improve the facility of carbonyl π–benzene π interaction between the polymeric stationary phase and PAH analytes.

2. Experimental

2.1. General methods and materials

L(−)phenylalanine (Wako, 99+%), γ-butyrolactone (Wako, 99+%), stearylamine (Wako 99%), *N*-carbobenzoxychloride (Z–Cl) (Wako, assay min 95%), diethyl phosphorocyanidate (DEPC) (Wako, assay min 90%) palladium carbon (Wako, Pd 5%) were used as-received. Triethylamine (Wako, 99+%) was distilled from potassium hydroxide. Trichlorosilane (TCA, 97%), 2-bromoisobutyryl bromide (Aldrich, 98%), 10-undecene-1-ol (Aldrich, 98%), platinum(0)-1,3-divinyl-1,1,3,3-tetramethyldisiloxane (Karstedt catalyst) (Aldrich, 0.1 M in xylenes), 1,1,4,7,7-pentamethyldiethylenetriamine (PMDETA) (Wako, 98.0%) and copper(I) bromide (Aldrich, 99.999%) were used as-received. Toluene (Wako, 99+%) and diethyl ether (Wako, 99.5+%) were distilled from sodium/benzophenone and stored under argon when not in use. Porous silica particles (YMC-GEL) were purchased from YMC Co. Ltd. (Kyoto, Japan) whose average diameter, pore size and surface area are 4 μm, 12 nm, and 300 $m^2 g^{-1}$, respectively. HPLC grade methanol as well as polycyclic aromatic hydrocarbon samples was obtained from Nacalai Tesque (Japan). IR measurements were conducted on a JASCO (Japan) FT/IR-4100 Plus instrument in KBr. For DRIFT measurement accessory DR PRO410-M (JASCO, Japan) was used. Thermogravimetric analyses were performed on a Seiko EXSTAR 6000 TG/DTA 6300 thermobalance in static air from 30 °C to 800 °C at a heating rate 10 °C min^{-1} using an empty crucible as reference. In order to remove solvent traces each sample was kept under vacuum at 35 °C for 5 h before analysis. Differential scanning calorimetric measurements (DSC) were carried out at a heating rate of 2 °C min^{-1} using a Seiko EXTRA 6000 with a DSC 6200 instrument and an empty pan as reference. In order to determine the bromine content of initiator-grafted silica particles the sample was combusted in Mitsubishi Chemical Analytech Automatic Burning Instrument (AQF-100) then the combustion gas was absorbed into a standard solution. The obtained solutions were analyzed by Dionex (ICS-2000) Ion Chromatograph using phosphorus as internal standard. A JCM 5700 scanning electron microscope was used for recording SEM images of the samples that were previously coated by osmium using Filgen Osmium Plasma Coater (OPC60A). The accelerating voltage of the SEM instrument was 5 kV and the emission current was 12 mA. Pore size measurements were carried out using Nova 2200e Surface Area and Pore Size Analyzer (outgas time: 3 h, outgas temperature: 21 °C, adsorbed gas: N_2, measurement temperature: 77.3 K, equilibrium time: 120 s, equilibrium timeout: 240 s). For characterization of organic compounds, ^{1}H and ^{13}C NMR spectra were recorded on a JEOL JNM-LA400 (Japan) instrument. Chemical shifts (δ) of ^{1}H, ^{13}C expressed in parts per million (ppm) with use of the internal standards Me_4Si ($\delta = 0.00$ ppm). Coupling constants (J) are reported in Hertz (Hz). Elemental analyses were carried out on a Perkin–Elmer CHNS/O 2400 apparatus. UV/vis spectra were measured on a JASCO V-560 spectrophotometer using quartz cell of 1 cm width.

2.2. Solid state NMR measurements (^{13}C CP/MAS NMR and ^{29}Si CP/MAS NMR)

NMR spectra were measured by Varian UnityInova AS400 at a static magnetic field of 9.4 T using solid probe for CP/MAS NMR at a spin rate 4000–4500 Hz. For solid state ^{13}C CP/MAS, the NMR measuring parameters are spectral width 50 000 Hz, proton pulse width PW 90 = 11.6 μs, contact time for cross-polarization 5 ms, and

delay before acquisition was 2 s. High-power proton decoupling of 63 db with fine attenuation of dipole $r = 2500$ was used only during detection periods. ^{29}Si cross-polarization magic angle spinning (CP-MAS) NMR spectra were collected with the same instrument. Representative samples of 200–250 mg were spun at 3500 Hz using 7 mm double bearing ZrO_2 rotors. The spectra were obtained with a cross-polarization contact time of 5 ms. The pulse interval time was 1.5 s. The transmitter frequency of ^{29}Si was 59.59 MHz. Typically, 1.5 k FIDs with an acquisition time of 30 ms were accumulated in 1 kb (kilobytes) data points and zero-filling to 8 kb prior to Fourier transformation. The line broadening used was 30 Hz and the spectral width for all spectra was about 25 kHz.

2.3. HPLC measurement

The chromatographic system consists of a Gulliver PU-980 intelligent HPLC pump with a Rheodyne sample injector having 20 μL loop. A JASCO multi-wavelength UV detector MD 2010 plus was used. The column temperature was maintained by using a column jacket with a circulator having a heating and a cooling system. A personal computer connected to the detector with JASCO-Borwin (Ver 1.5) software was used for system control and data analysis. As the sensitivity of UV detector is high, 5 μL of sample solution was used for each injection. To avoid overloading effects, special attention was given in this study to the selection of optimum experimental conditions. Separations were performed using HPLC grade methanol and water mixture (90:10) as mobile phase at a flow rate 1.00 mL min^{-1}. The measurements were done under isocratic elution conditions and retention factors (k) were defined by $(t_r - t_0)/t_0$ where t_0 and t_r are the retention times of methanol and samples respectively. The separation factor (α) is the ratio of the retention factor of two solutes that are being analyzed ($\alpha = k_2/k_1$). Retention time of D_2O was used as the void volume (t_0) marker (the absorption for D_2O was measured at 400 nm, which actually considered as injection shock). All data points were derived from at least triplicate measurements; with retention time (t_R) value varying ±1%. Water/1-octanol partition coefficient (P) was measured by the retention studies with octadecylated silica, ODS (monomeric) (Inertsil ODS, i.d. 250 × 4.6 mm, GL Science, Tokyo, Japan): $\log P = 3.759 + 4.203 \log k$ ($r = 0.999997$).

2.4. Synthesis of L-phenylalanine-derived monomer

N′-Octadecyl-L-phenylalanineamide (**1**) was synthesized according to a previously reported method [28].

2.4.1. N′-Octadecyl-N$^{\alpha}$[4-(hydroxy)-butanoyl]-L-phenylalanineamide (**2**)

Compound **1** (7.50 g, 18.0 mmol) was mixed with γ-butyrolactone (85 mL), stirred and refluxed for 72 h in oil bath. The mixture was cooled to room temperature and 500 mL acetonitrile was added and the solution was stored at −20 °C for 6 h. The white precipitate was filtered, washed with acetonitrile several times and dried in vacuo giving **2** (7.74 g, 85.6%). M.p. 78–81 °C; elemental analysis calcd (%) for $C_{31}H_{54}N_2O_3$: C 74.05, H 10.83, N 5.57; found C 74.85, H 10.83, N 5.79; FTIR (KBr)/cm^{-1} 3287, 2917, 2849, 1635, 1567, 1536, 1470, 1163, 1061; ^{1}H NMR (400 MHz, $CDCl_3$) δ 7.25 (5H, m, C_6H_5), 6.32 (1H, d, $J = 6.84$ Hz, N*H*C(O)*CH), 4.37 (1H, t, $J = 14.64$ Hz, *C*H*), 3.66 (2H, m, –C*H*$_2$OH), 3.25 (2H, m, *CHC*H*$_2$C$_6$H$_5$), 3.10 (2H, m, C*H*$_2$NHC(O)*CH), 3.07 (2H, m, *CHNHC(O)C*H*$_2$), 2.36 (2H, t, $J = 12.0$ Hz, –CH$_2$C*H*$_2$(O)H), 1.25 (33H, m, CH$_3$C*H*$_2$ × 16), 0.86 (3H, t, $J = 12.0$ Hz, –C*H*$_3$); ^{13}C NMR (100 MHz, $CDCl_3$) δ 174.03, 173.27, 170.56, 138.02, 136.76, 129.31, 129.26, 128.69, 127.05, 126.78, 62.56, 56.50 54.80, 41.11, 39.585, 38.86, 32.66, 31.90, 29.68, 29.64, 29.58, 29.48, 29.34, 29.25, 29.21, 26.92, 26.77, 24.60, 22.70, 14.13.

2.4.2. N′-Octadecyl-N$^{\alpha}$[4-(acryloyloxy)-butanoyl]-L-phenylalanineamide (**3**)

Compound **2** (7.5 g, 14.91 mmol) was dissolved in anhydrous THF (300 mL) by stirring. Anhydrous triethylamine (4.52 g, 44.75 mmol) was added into the mixture and the temperature was maintained at 0 °C with ice bath. Acryloyl chloride (2.71 g, 30.0 mmol) in 10.0 mL anhydrous THF was added drop wise and the reaction mixture was stirred at 0 °C for 1 h. The mixture was then let warm to room temperature and stirring was continued for another 12 h to complete acylation reaction. After 12 h triethylammonium chloride was removed by filtration, the filtrate was concentrated under vacuum and dissolved in $CHCl_3$ (250 mL). The chloroform solution was washed with 10% $NaHCO_3$ solution, 0.2 M HCl and distilled water. The solution was dried over Na_2SO_4, concentrated under reduced pressure, recrystallized from methanol and dried in vacuo giving **3** as white powder (6.42 g, 77.4%). M.p. 82–85 °C; elemental analysis calcd (%) for $C_{34}H_{56}N_2O_4$: C 73.33, H 10.13, N 5.03; found C 70.65, H 9.85, N 4.91; FTIR (KBr)/cm^{-1} 3287, 2918, 2849, 1727, 1638, 1559, 1466, 1195; ^{1}H NMR (400 MHz, $CDCl_3$) δ 7.20 (5H, m, C_6H_5), 6.37 (1H, q, $J = 16.44$ Hz, –CH=C(H)*H*), 6.26 (1H, d, $J = 8.76$ Hz, –CH$_2$–N*H*–C(O)–*CH), 6.07 (1H, q, $J = 28.32$ Hz, –C*H*=CH$_2$), 5.85 (1H, d, $J = 10.76$ Hz, –CH=C(*H*)H), 5.51 (1H, s, –*CH–N*H*–C(O)), 4.52 (1H, m, –*C*H*), 4.11 (2H, m, –CH$_2$–CH$_2$–C*H*$_2$–O–C(O)), 3.10 (2H, m, C*H*$_2$NHC(O)*CH), 2.95 (2H, m, *CHC*H*$_2$C$_6$H$_5$), 2.25 (2H, t, $J = 14.64$ Hz, –NH–C(O)–C*H*$_2$–CH$_2$–), 1.96 (2H, q, $J = 24$ Hz, –NH–C(O)–CH$_2$–C*H*$_2$–), 1.25 (32H, m, CH$_3$C*H*$_2$ × 16), 0.86 (3H, t, $J = 12.0$ Hz, C*H*$_3$); ^{13}C NMR (100 MHz, $CDCl_3$) δ 171.66, 170.5152, 166.15, 136.80, 130.84, 129.24, 128.66, 128.33, 127.01, 63.47, 54.80, 39.55, 38.86, 32.66, 31.90, 29.68, 29.64, 29.58, 29.48, 29.34, 29.25, 29.21, 26.92, 26.77, 24.60, 22.67, 14.08.

2.5. Surface-initiated ATRP of monomer **3** from Sil-**4**

[11-(2-Bromo-2-methyl)propionyloxy]undecyltrichlorosilane (**4**) was immobilized onto silica by the reaction between trichlorosilyl anchoring groups and surface silanol groups giving initiator-modified silica (Sil-**4**) [28]. Sil-**4** (4.1 g), compound **3** (4.01 g, 7.2 mmol) and PMDETA (0.410 g, 2.366 mmol) were weighed on a round-bottomed flask then dry toluene (17 mL) was added and the suspension was purged with nitrogen. After the addition of CuBr (0.2214 g, 1.543 mmol) the mixture was deoxygenated (three freeze-vacuum-N_2 cycles). The flask was then immersed into an oil bath (90 °C) and rotated at a slow velocity for 24 h. Toluene was added, the reaction mixture was cooled to room temperature and filtered. Poly**3**-silica composite was repeatedly re-suspended in hot organic solvents (toluene, chloroform and methanol) and filtered several times to remove nonbonded monomers. The particles were placed in a round-bottomed flask, suspended in a mixture of methanol and an aqueous solution of K_2EDTA (0.25 M) [30] and then the flask was rotated at 40 °C for 6 h to eliminate catalyst traces. The suspension was filtered and the residue was washed with water, methanol, and diethyl ether giving Sil-poly**3**.

3. Results and discussion

3.1. Synthesis of monomer **3**

Compounds **2** and **3** have been prepared according to the synthetic process that is illustrated in Fig. 1. The reaction between *N′*-octadecyl-L-phenylalanineamide [28] (**1**) and γ-butyrolactone resulted in the formation of *N′*-octadecyl-*N*$^{\alpha}$[4-(hydroxy)-butanoyl]-L-phenylalanineamide (**2**). The hydroxyl group in compound **2** was acylated by acryloyl chloride in the presence of anhydrous triethylamine giving *N′*-octadecyl-*N*$^{\alpha}$[4-(acryloyloxy)-butanoyl]-L-phenylalanineamide (**3**) as white powder. Compounds **2** and **3** were

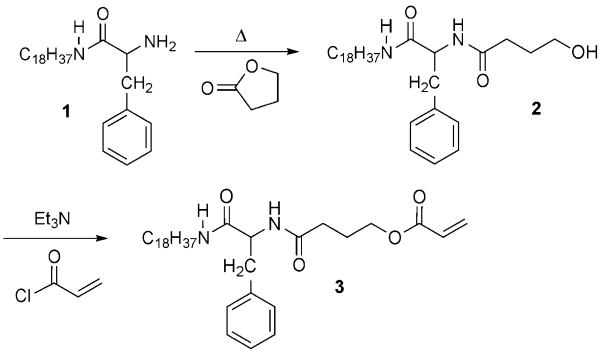

Fig. 1. Synthesis of compound **3**.

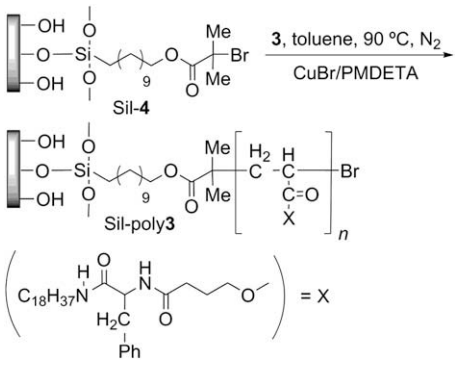

Fig. 3. Preparation of poly**3**-grafted silica particles (Sil-poly**3**).

characterized by elemental analysis and different spectroscopic methods (^{1}H NMR, ^{13}C NMR and FTIR) as summarized in Section 2. ^{1}H NMR and ^{13}C NMR spectra of monomer **3** are shown in Figs. S1 and S2 in Supporting data.

The ordered structural conformation of the alkyl chains of monomer **3** was evaluated by ^{13}C CP/MAS NMR measurement (Fig. 2 (inset)). The high intensity of peak at 33.4 ppm due to *trans*-conformation and the absence of peak attributed to *gauche* conformation revealed the domination of rigid, ordered chains over the mobile amorphous regions [31].

3.2. Surface-initiated ATRP of **3** from silica

The preparation of poly**3**-grafted silica particles has been carried out in two steps: (1) attachment of ATRP initiator onto silica surface and (2) subsequent polymerization of **3** from initiator-modified silica (Fig. 3). [11-(2-Bromo-2-methyl)propionyloxy]undecyltrichlorosilane [32] (**4**) radical initiator was grafted onto silica using a previously reported method [28]. ATRP initiator (**4**) consists of three basic components: an anchoring group (–$SiCl_3$) linking the initiator to the surface, a cleavable group (–O–C═O) and an α-bromo group that undergoes the reversible halogen atom transfer reaction. ATRP of **3** from initiator-grafted silica was conducted in dry toluene under nitrogen atmosphere in the presence of CuBr and 1,1,4,7,7-pentamethyldiethylenetriamine (PMDETA) as catalyst precursors

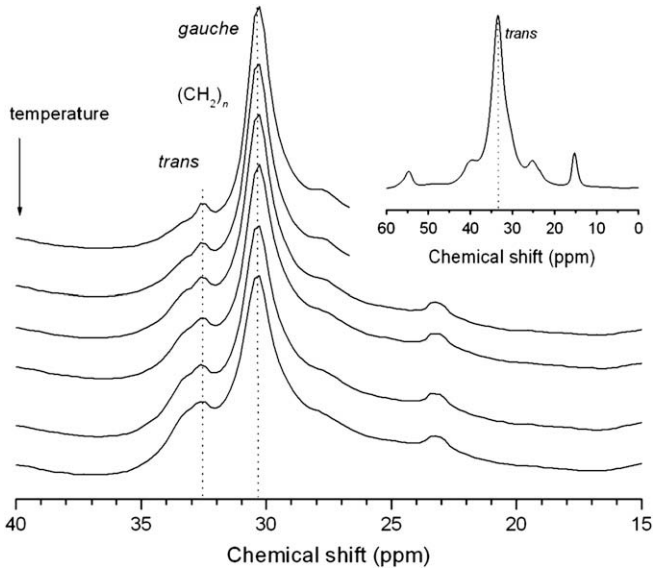

Fig. 2. Partial ^{13}C CP/MAS NMR spectra of monomer **3** (inset) and Sil-poly**3** in the temperature range from 50 to 25 °C.

(see Section 2). The particles were filtered and washed free of any absorbed monomer with several cycles of filtration and re-suspension in hot organic solvents (toluene, $CHCl_3$ and MeOH) and then volatile compounds were evaporated under vacuum. Sil-poly**3** was characterized by elemental analysis, different spectroscopic methods (DRIFT, NMR), thermogravimetric analysis (TGA) and differential scanning calorimetry (DSC).

3.3. Characterization of the silica composites

Weight percentage of grafted phase (P_w) and surface coverage of Sil-poly**3** were calculated [33] from elemental analysis data (C: 26.6%; H: 4.17%; N: 1.64%) as 22.9 wt% and 1.76 μmol m^{-2} respectively.

Thermogravimetric analysis (TGA) easily monitors the amount of poly**3** attached to silica cores. The heating process was carried out up to 800 °C which has been demonstrated to be sufficiently high to degrade all surface-bonded organosilanes [34]. Fig. S3 shows the TGA curves of untreated bare silica particles (a) with the weight loss of 7.2 wt% due to the loss of water molecules absorbed to the surface. Curve (b) shows 9.6 wt% difference [28] between the weight retention of **4** initiator-grafted silica (83.2 wt%) and bare silica (92.8 wt%) indicating that fairly high amount of initiator could be immobilized. However, the translation of this weight difference into grafting density may lead to false value because surface modification altered the hydrophobicity of silica surface, consequently, bare silica contains more adsorbed water than Sil-**4**. Instead, grafting density of initiator **4** was determined on the basis of Br content of Sil-**4** (4.05 wt%) giving 605 μmol g^{-1}. Thermogravimetric investigation revealed that Sil-poly**3** lost 39.4 wt% of its original weight up to 600 °C showing two main areas of thermal decomposition, the first from 240 to 350 °C and the second one from 390 to 600 °C. The existence of a plateau in the weight retention profile of Sil-poly**3** at 600 °C confirms that there is no volatile material remained on the silica. If the weight retention of Sil-**4** was considered as reference, the weight of the grafted poly**3** could be calculated as 22.6 wt% of the total mass. This value corresponds to the weight percentage of the grafted organic phase (P_w) calculated on the basis of elemental analysis (22.9 wt%). TGA measurements helped to obtain information about the effectiveness of initiator immobilization and surface-initiated polymerization of compound **3**.

Presence of grafted polymer on silica particles can also be confirmed by diffuse reflectance infrared Fourier transform (DRIFT) spectroscopy. Fig. S4 shows the DRIFT spectra, for bare silica (a), Sil-**4** (b), Sil-poly**3** (c) and the FTIR spectrum of monomer **3** (d) in the range from 3450 to 1590 cm^{-1}. For initiator-grafted silica, characteristic bands were detected at 2928, 2857 and 1717 cm^{-1} attributed to $\nu_{as}(CH_2)$, $\nu_s(CH_2)$ and ν(C═O) respectively [28]. DRIFT

spectrum of Sil-poly**3** demonstrated broad signals at 3285, 1731 and 1640 cm^{-1}. These bands are assigned to N–H stretching, ester carbonyl stretching and amide carbonyl stretching respectively.

Furthermore, a group of peaks with low intensity arisen from aromatic C–H stretching could be detected at 3066 cm^{-1}. These observations are in good agreement with the results obtained by TGA measurements confirming the presence of grafted poly**3** on the silica surface.

Solid state ^{13}C cross-polarization magic angle spinning (CP/MAS) NMR provides useful information of the chemical composition of modified surfaces furthermore gives evidence about conformation and dynamics of immobilized alkyl groups [31,35]. Generally, different conformations of the alkyl chain are visible in the two signals of the $(CH_2)_n$ chains at 32.6 and 30.0 ppm due to *trans* and *gauche* conformations respectively [36]. While *trans* conformations indicate rigid, ordered chains; the *gauche* conformations characterize mobile, amorphous regions. ^{13}C CP/MAS NMR spectra of Sil-poly**3** were recorded at variable temperatures (50–25 °C) to gain insight into the conformation of octadecyl chains (Fig. 2). Looking at the spectrum acquired at 50 °C, intense signal attributed to *gauche* conformation can be seen at 30.2 ppm while the intensity of signal at 32.6 ppm due to the *trans* conformation is very low. Usually, when the temperature is decreasing more *trans* conformations are formed because of lower mobility of the alkyl chains. Surprisingly, at lower temperature (25 °C) the *trans–gauche* ratio remained the same as it was observed at 50 °C, in other words higher fraction of immobilized $(CH_2)_n$ chains in poly**3** are amorphous and mobile while self-assembling of monomer **3** could be observed at ambient temperature. The fact that the *trans–gauche* ratio is independent on the temperature is supported by the lack of phase transition that usually can be observed by differential scanning calorimetry (DSC) [37]. DSC curve of Sil-poly**3**/MeOH/H_2O mixture is shown in Fig. S5.

^{29}Si CP/MAS NMR spectroscopy is well suited for assessing the presence of different silicon species in polymer-layered silica particles. Resonances for the silica species appear separately between −50 and −125 ppm as shown in Fig. S6. Intense signals at −111.5 and −102.5 ppm in the spectrum of Sil-**4** can be attributed to siloxane bridges (Q^4) and vicinal (Q^3) silanol groups while the signal with low intensity at −91.7 ppm is due to geminal silanol groups (Q^2) [38]. ^{29}Si CP/MAS NMR measurement of Sil-**4** also revealed the presence of T^2 species (−55.8 ppm) indicating that not all chlorosilane groups reacted with the surface silanol groups rather the hydrolysis of those groups resulted in Si–OH functionalities. Appearance of T^3 species (−65.7 ppm) in the spectrum of Sil-poly**3** can be explained by the (poly)condensation of Si–OH moieties under the conditions of ATRP reaction giving siloxane-bridged organic layer. Illustration of different silicon containing species is given in Fig. S7.

Pore size of Sil-**4** and Sil-poly**3** was determined by nitrogen gas adsorption–desorption method (6.04 and 1.71 nm, respectively) providing evidence that the pore radius of silica particles significantly decreased during the polymerization. The transmission electron microscopy (TEM) micrographs of **4** initiator-modified and polymer-grafted silica microspheres as shown in Fig. 4 indicated that polymer grafting did not affect the particle size (4.08 and 4.10 μm respectively), furthermore that particles remained unagglomerated. Unagglomerated polymer-grafted silica particles (Sil-poly**3**) were found suitable for chromatographic stationary phase, and packed into stainless steel column.

3.4. Chromatographic performance

Sil-poly**3** as a new stationary phase was initially tested with a mixture containing uracil, toluene and naphthalene. The column provided the separation factors (defined in Section 2) of 1.22 between toluene and uracil and 1.19 between naphthalene and toluene using methanol as a mobile phase with an optimal flow rate of 1.0 mL min^{-1}. The chromatogram is shown in Fig. 5.

Additionally, chromatographic performance of Sil-poly**3** was compared with monomeric octadecylsilane (ODS-m) [28], Sil-poly(Phe-St) [28], poly(L-alanine)-grafted silica (Sil-Ala_n) [39], poly(octadecyl acrylate)-grafted silica (Sil-ODA_n) [32] and poly(4-vinyl pyridine)-grafted silica (Sil-VP_n) [29] columns to investigate how structural modification of the applied monomer affects the molecular recognition ability.

The comparison between the retention behavior of alkylbenzenes and PAHs may be used to evaluate the retention mode of packing materials in HPLC [40]. It is well known that $\log P = 3.759 + 4.203 \log k$ equation [41] describes the relation between partition coefficient (P) and retention factor (k) in reversed-phase HPLC when the elevated retention of a certain analyte can be clearly explained on the basis of its higher hydrophobicity. Contrarily, if the slope of log P *versus* log k plot is higher than 4.203 it indicates that other type of interactions (e.g. carbonyl π–benzene π) also contribute to the retention of the analyte. Fig. 6 shows the relationship between log k and log P with Sil-poly**3** and monomeric octadecylsilane (ODS-m) columns. (Determination of partition coefficients (P) is described in Section 2.) As depicted in Fig. 6, Sil-poly**3** showed relatively lower retention for alkylbenzenes than ODS-m. Interestingly, the log P–log k plots showed similar slopes for both alkylbenzenes and PAHs in ODS-m while those obtained by Sil-poly**3**, significantly differ from each other. On the other hand, the separation factors (α), namely the ratio between the retention factors for two alkylbenzenes are fairly closed to each other in ODS-m and in Sil-poly**3**. For example, the separation factors between dodecyl- and decylbenzenes were 1.31 in Sil-poly**3** and 1.26 in ODS-m. This resembles a reversed-phase mode which shows slightly higher separation for alkylbenzenes by Sil-poly**3** than ODS-m. However, naphthacene and anthracene show a separation factor of 2.17 for Sil-poly**3** while it lies 1.78 for ODS-m which proves the higher selectivity for PAHs on Sil-poly**3**. The extremely enhanced selectivity for PAHs on Sil-poly**3** provides us information about its specific interactive sites for PAHs like Sil-ODA_n [42]. We have also observed that Sil-poly**3** yielded much higher retention for PAHs compared to its value for alkylbenzenes. For instance, the log P of naphthacene (5.71) is much smaller than dodecylbenzene (8.43), but the log k value of naphthacene (1.22) is higher than that of dodecylbenzene (0.98) further prove its higher selectivity towards PAHs. The retention and separation factors of some PAHs and aromatic positional isomers are given in Table 1 with the data obtained for ODS-m. Molecular shape recognition ability of poly**3** was investigated by separation of mixtures containing linear and non-linear furthermore planar and non-planar PAHs. Structures of the applied analytes are shown in Fig. S8. In order to find experimental evidence for the linearity recognition capability of Sil-poly**3**, the separation factor for naphthacene and triphenylene ($\alpha_{naphthacene/triphenylene}$) was determined and enhanced separation was found in the case of Sil-poly**3** (1.62) compared with ODS-m (1.23). Both naphthacene and triphenylene possess the same molecular weight consequently the mechanism of their separation must be explained by having different geometries rather than by the difference between their hydrophobicities. Hence, the separation factor, $\alpha_{naphthacene/triphenylene}$, between the two analytes, can be regarded as a quantitative index of shape selectivity. It is particularly noteworthy that $\alpha_{naphthacene/triphenylene}$ was lower (1.33) with Sil-poly(Phe-St) indicating the better linearity recognition of Sil-poly**3**. This findings fit well to our previously reported results namely the linearity selectivity of Sil-poly**3** is much better than Sil-VP_n however it is worse than that was observed with β-structural Sil-Ala_n ($\alpha_{naphthacene/triphenylene} = 5.74$) [39]. To extend the linearity recognition studies to the investigation of molecular planarity

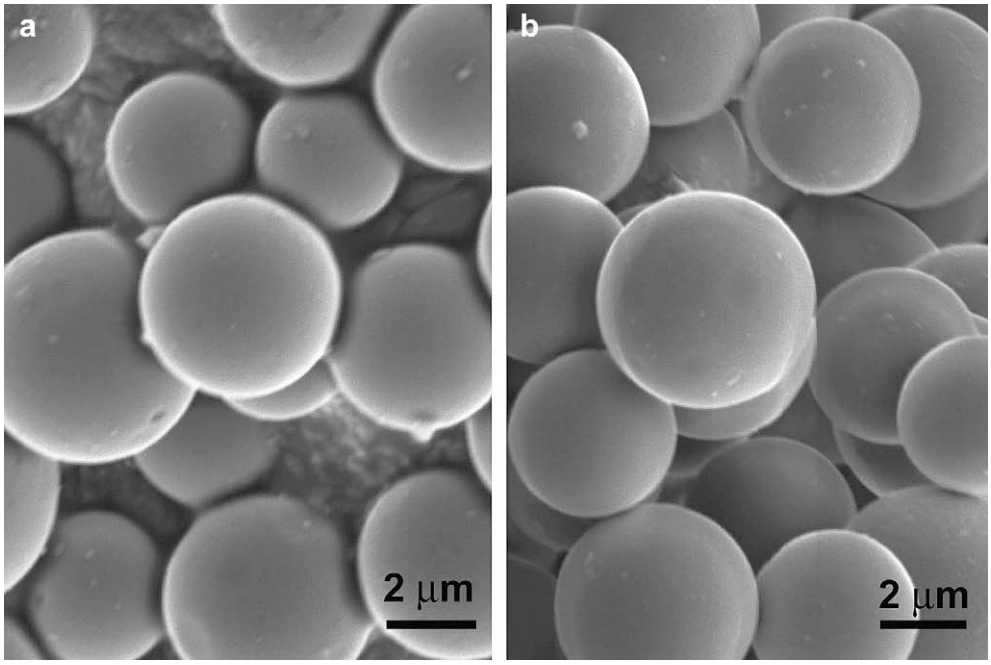

Fig. 4. SEM images of (a) Sil-**4** and (b) Sil-poly**3**.

recognition we determined the separation factor for *p*-terphenyl and *o*-terphenyl ($\alpha_{p\text{-terphenyl}/o\text{-terphenyl}}$) as an indicator of the ability to detect planarity of analytes. Both *p*- and *o*-terphenyl have the same number of carbon atoms and π-electrons, but the molecular planarity is entirely different: while *p*-terphenyl is a little twisted (almost planar) *o*-terphenyl is a non-planar compound. Poly**3** stationary phase showed enhanced selectivity ($\alpha_{p\text{-terphenyl}/o\text{-terphenyl}} = 2.21$) towards test mixture containing all positional isomers of terphenyl compared with monomeric ODS. As it is indicated in Table 1 chromatographic separation of terphenyl isomers with ODS-m resulted in significantly lower separation factor ($\alpha_{p\text{-terphenyl}/o\text{-terphenyl}} = 1.44$) moreover, did not discriminate between *m*- and *p*-isomers. The differences in linearity- and planarity recognition ability of ODS-m and Sil-poly**3** are undoubtedly attributed to the fact that latter involves three carbonyl groups per monomer unit providing a facility for carbonyl π interaction besides hydrophobic effect. Not surprisingly, the planarity selectivity of Sil-poly**3** and Sil-poly(Phe-St) was found practically the same for the separation of triphenylene/*o*-terphenyl analytes, 3.17 and 3.23 respectively, because both organic phases are mainly disordered as it was proven by ^{13}C CP/MAS NMR spectra. It must be added here that while Sil-Ala$_n$ provided significantly lower separation factor for planar and non-planar analytes ($\alpha_{\text{triphenylene}/o\text{-terphenyl}} = 1.37$), extremely high planarity selectivity (9.85) was observed with Sil-VP$_n$.

Important conclusions related to the molecular recognition ability of the newly developed stationary phase can be drawn from the chromatographic performance and the conformational studies

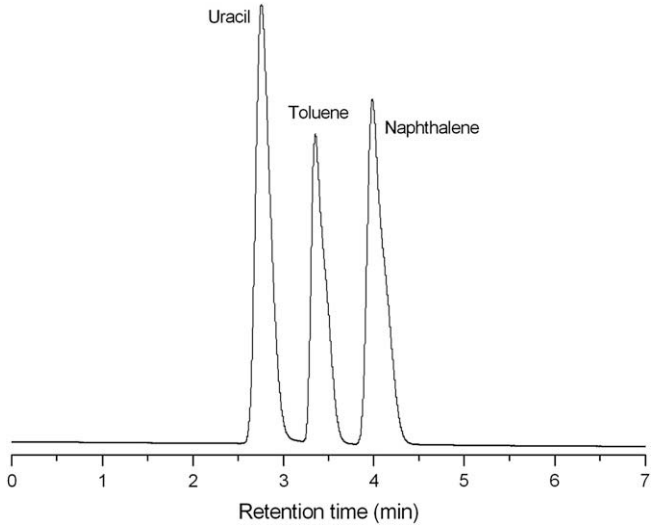

Fig. 5. Chromatogram for a mixture of uracil, toluene and naphthalene with Sil-poly**3** column. Mobile phase: methanol–water (90:10) at a flow rate 1 mL min^{-1}, column temperature: 25 °C, UV detection (254 nm). Column 4.6 ID × 250 mm.

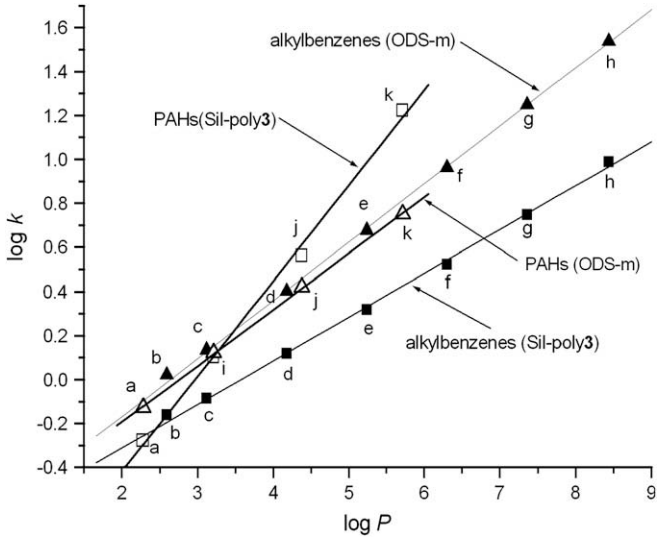

Fig. 6. Log *k* *versus* log *P* for ODS-m and Sil-poly**3** stationary phases; a: benzene, b: toluene, c: Et-benzene, d: Bu-benzene, e: hexylbenzene, f: octylbenzene, g: decylbenzene, h: dodecylbenzene, i: naphthalene, j: anthracene, k: naphthacene. Mobile phase: methanol–water (90:10) at a flow rate 1 mL min^{-1}, column temperature: 30 °C, UV detection (254 nm).

Table 1
Retention and separation factors of PAHs for Sil-poly**3**, Sil-poly(Phe-St) and ODS-m stationary phases.

Analyte[a]	Sil-poly**3**		Sil-poly (Phe-St) [28]		ODS-m [28]	
	k	*α*	*k*	*α*	*k*	*α*
Benzene	0.57		0.974		0.74	
		2.09		2.36		1.78
Naphthalene	1.19		2.30		1.32	
		5.42		6.30		3.55
Anthracene	3.09		6.14		2.63	
Pyrene	4.72		10.28		3.76	
		1.55		1.41		1.21
Triphenylene	7.32		14.42		4.57	
		1.66		1.23		1.29
Benzo[*a*]anthracene	7.84		12.64		4.87	
		1.74		1.43		1.30
Chrysene	8.21		14.70		4.89	
		2.52		1.90		1.49
Naphthacene	11.88		19.10		5.60	
o-Terphenyl	2.31		4.47		3.07	
		1.77		1.95		1.44
m-Terphenyl	4.10		8.71		4.45	
		2.21		3.10		1.44
p-Terphenyl	5.101		13.81		4.45	

[a] Mobile phase: methanol–water (90:10) at a flow rate 1 mL min^{-1}, column temperature: 30 °C, UV detection (254 nm).

of Sil-poly**3**: (1) although the majority of octadecyl chains are in disordered conformation in Sil-poly**3** the presence of propyleneoxycarbonyl spacer instead of *p*-phenylene group in the monomer resulted in significant enhancement of linearity selectivity towards PAHs, (2) although higher retention factors were observed with poly(Phe-St), owing to the presence of one more benzene ring in every monomer unit providing higher hydrophobicity, Sil-poly**3** shows better linearity selectivity. At first the linearity selectivity results might appear contradictory, however if one compare the energy of these interactions, one will see that carbonyl π–benzene π interaction [42] is stronger than benzene π–benzene π interaction [43] consequently it must have higher effect on the linearity selectivity.

4. Conclusions

A novel L-phenylalanine-based monomer; *N*′-octadecyl-*N*$^{\alpha}$-[4-(acryloyloxy)-butanoyl]-L-phenylalanineamide (**3**) has been synthesized, and its self-assembling properties were investigated by FTIR and variable temperature ^{1}H NMR spectroscopy. It was found that hydrogen bonding between the carbonyl- and amide groups, furthermore weak van der Waals interactions between the octadecyl chains is responsible for the self-assembly of monomer **3**. Surface-initiated atom transfer radical polymerization of compound **3** has been carried out from initiator-grafted porous silica gel to immobilize molecular shape recognitive polymer. The results of thermogravimetric and diffuse reflectance infrared Fourier transform spectroscopic analyses revealed that fairly large amount of polymer could be attached to silica surface. ^{13}C CP/MAS NMR measurement of the inorganic–polymer hybrid material (Sil-poly**3**) demonstrated that octadecyl chains of the grafted polymer are in less ordered *gauche* conformational form. Poly**3**-grafted particles were used as separation materials for reversed-phase high performance liquid chromatography. It was found that Sil-poly**3** shows significantly better molecular shape and planarity recognition for polycyclic aromatic hydrocarbons than ODS-m column while the comparison of chromatographic performance of Sil-poly(Phe-St) and Sil-poly**3** led us conclude that substitution of *p*-phenylene spacer by propyleneoxycarbonyl group not only reduced the retention time but also increased the linearity recognition.

Acknowledgement

This work was partially supported by Grant-in-Aid for Scientific Research from the Ministry of Education, Culture, Sports, Science and Technology of Japan.

Appendix. Supporting data

Supplementary data associated with this article, can be found, in the on line version at doi:10.1016/j.polymer.2008.10.017.

References

[1] Alivisatos AP. Science 1996;271:933.
[2] Advincula Rc. J Dispersion Sci Technol 2003;24:343.
[3] Schauwecker B, Arnold M, Radehaus CV, Przyrembel G, Kuhlow B. Opt Eng 2002;41:237.
[4] Philipse S, van Bruggen MPB, Pathmamanoharan C. Langmuir 1994;10:92.
[5] El-Nahhal IM, El-Ashgar NM. J Org Chem 2007;692:2861.
[6] Pharm KN, Fullston D, Sagoe-Crentsil K. J Colloid Interface Sci 2007;315:123.
[7] Besteman K, Lee J, Wiertz F, Heering H, Dekker C. Nano Lett 2003;3:727.
[8] Eastmond G, Nguyen-Huu C, Piret W. Polymer 1980;21:598.
[9] Ihara H, Okazaki S, Ohmori K, Uemura S, Hirayama C, Nagaoka S. Anal Sci 1998;14:349.
[10] Halperin A, Tirrell M, Lodge TP. Adv Polym Sci 1992;100:31.
[11] Hadziioannou G, Patel S, Granick S, Tirrell M. J Am Chem Soc 1986;108:2869.
[12] Reiter G. Europhys Lett 1996;33:29.
[13] Krenkler KP, Laible R, Hamann K. Angew Macromol Chem 1953;53:101.
[14] Hosoya M, Yanadori K, Sone Y. Macromol Sci Chem 1990;A27:445.
[15] Takafuji M, Ide S, Ihara H, Xu Z. Chem Mater 2004;16:1977.
[16] Zajac R, Chakrabarti A. Phys Rev E 1995;52:6536.
[17] Ulman A. Chem Rev 1996;96:1533.
[18] Cossement D, Mekhalif Z, Delhalle J, Hevesi L. In: Auner N, Weis J, editors. Organosilicon chemistry VI, vol. 1. Weinheim: Wiley-VCH; 2005. p. 999.
[19] Prucker O, Rühe J. Langmuir 1998;14:6893.
[20] Hemström P, Szumski M, Irgum K. Anal Chem 2006;78:7098.
[21] Matyjaszewski K, Spanswick KJ. Mater Today 2005;8:26.
[22] Kamigaito M, Ando T, Sawamoto M. Chem Rev 2001;101:3689.
[23] Matyjaszewski K. Controlled/living radical polymerization: progress in ATRP, NMP and RAFT, ACS Symposium Series, vol. 768. Washington, DC: American Chemical Society; 2000.
[24] Cléchet P, Martelet C, Belin M, Zarrad H, Jaffrezic-Renault N, Fayeulle S. Sens Actuators A Phys 1994;44:77.
[25] Ihara H, Shundo A, Takafuji M, Nagaoka S. In: Cazes J, editor. Encyclopedia of chromatography. London: Taylor & Francis; 2007. p. 1.
[26] Ohmact R, Kele M, Matus Z. Chromatographia 1994;39:668.
[27] Ihara H, Goto Y, Sakurai T, Takafuji M, Sagawa T, Nagaoka S. Chem Lett 2001;12:1252.
[28] Rahman MM, Czaun M, Takafuji M, Ihara H. Chem Eur J 2008;14:1312.
[29] Gautam UG, Shundo A, Gautam MP, Takafuji M, Ihara H. J Chromatogr A 2008;1189:77.
[30] Shen Y, Tang H, Ding S. Prog Polym Sci 2004;29:1053.
[31] Pursch M, Sander LC, Händel H, Albert K. Anal Chem 1996;68:4107.
[32] Matyjaszewski K, Miller PJ, Shukla N, Immaraporn B, Gelman A, Luokala BB, et al. Macromolecules 1999;32:8716.
[33] Ansarian HR, Derakhshan M, Rahman MM, Sakurai T, Takafuji M, Ihara H. Anal Chim Acta 2005;547:179.
[34] Chamberg M, Parnas R, Cohen Y. J Appl Polym Sci 1989;37:2921.
[35] Pursch M, Strohschein S, Händel H, Albert K. Anal Chem 1996;68:386.
[36] Albert K, Schmid J, Pfleiderer B, Bayer E. Chemically modified surfaces, vol. 4. Amsterdam: Elsevier Science Publishers; 1992. pp. 105.
[37] Mallik AK, Rahman MM, Czaun M, Takafuji M, Ihara H. Chem Lett 2007;36:1460.
[38] Albert K, Bayer E. J Chromatogr 1991;544:345.
[39] Shundo A, Sakurai T, Takafuji M, Nagaoka N, Ihara H. J Chromatogr A 2005;1073:169.
[40] Ihara H, Dong W, Mimaki T, Nishihara M, Sakurai T, Takafuji M, et al. J Liq Chromatogr 2003;26:2473.
[41] Rekker RF, de Kort HM. Eur J Med Chem 1979;14:479.
[42] Goto Y, Nakashima K, Mitsushi K, Takafuji M, Sakaki S, Ihara H. Chromatographia 2002;56:19.
[43] Sakaki S, Kato K, Miyazaki T, Musashi Y, Ohkubo K, Ihara H, et al. J Chem Soc Faraday Trans 2 1993;9:659.